THE ANATOMICAL RECORD 292:1720–1733 (2009)

Climate Signatures in the Morphological Differentiation of Worldwide Modern Human Populations

MARK HUBBE,[1] TSUNEHIKO HANIHARA,[2] AND KATERINA HARVATI[3,4]*
[1]Instituto de Investigaciones Arqueológicas y Museo, Universidad Católica del Norte, San Pedro de Atacama, Chile
[2]Department of Anatomy, Kitasato University School of Medicine, Sagamihara, Japan
[3]Department of Human Evolution, Max Planck Institute for Evolutionary Anthropology, Leipzig, Germany
[4]Department of Early Prehistory and Quaternary Ecology, University of Tübingen, Tübingen, Germany

ABSTRACT

The ability of cranial morphology to reflect population/phylogenetic history, and the degree to which it might be influenced by environmental factors and selection pressures have been widely discussed. Recent consensus views cranial morphology as largely indicative of population history in humans, with some anatomical cranial regions/measurements being more informative on population history, while others being under selection pressure. We test earlier findings using the largest and most diverse cranial dataset available as yet: 7,423 male specimens from 135 geographic human population samples represented by 33 standard craniometric linear measurements. We calculated Mahalanobis D^2 for three datasets: complete cranial dataset; facial measurement dataset; and neurocranial measurement dataset; these morphological distance matrices were then compared to matrices of geographic distances as well as of several climatic variables. Additionally, we calculated Fst values for our cranial measurements and compared the results to the expected Fst values for neutral genetic loci. Our findings support the hypothesis that cranial, and especially neurocranial morphology, is phylogenetically informative, and that aspects of the face and cranium are subject to selection related to climatic factors. The Fst analysis suggest that selection to climate is largely restricted to groups living in extremely cold environments, including Northeast Asia, North America, and Northern Europe, though each of these regions appears to have arrived at their morphology through distinct adaptive pathways. Anat Rec, 292:1720–1733, 2009.

Key words: Fst; craniometrics; adaptation; population history; human variation; Neanderthals

The degree to which human cranial morphology reflects population history or adaptive and developmental changes related to environmental conditions is the subject of ongoing scientific discussion in anthropology. Our understanding of the evolutionary processes affecting morphological variation directly impacts both the study of modern human geographic diversity as well as the interpretation of the human fossil record. The relevance of cranial morphology to phylogenetic reconstruction has been questioned in the past (see e.g., Collard and Wood, 2000), and convergence, parallelism, reversals, and environmen-

Grant sponsor: FONDECYT; Grant number: 11070091; Grant sponsor: Marie Curie Research Training Network; Grant number: MRTN-CT-019564; Grant sponsor: Max Planck Gesellschaft.

*Correspondence to: Katerina Harvati, Department of Early Prehistory and Quaternary Ecology, University of Tübingen, Rümelinstrasse 19-23, 72070 Tübingen, Germany. Fax: +49-7071-295717. E-mail: harvati@eva.mpg.de

Received 27 March 2009; Accepted 8 June 2009

DOI 10.1002/ar.20976
Published online 28 August 2009 in Wiley InterScience (www.interscience.wiley.com).

tal plasticity are commonly cited as obscuring any phylogenetic signal that it may preserve. The effects of mastication and climatic adaptation on the cranium are thought to be particularly extensive, with some anatomical regions or measurements believed to be affected differentially by these processes (e.g., Hylander, 1977; Carey and Steegmann, 1981; Olson, 1981; Beals et al., 1983; Skelton and McHenry, 1992; Larsen, 1999; Wood and Lieberman, 2001; Lieberman et al., 2004; Roseman, 2004; Roseman and Weaver, 2004; González-José et al., 2005; Harvati and Weaver, 2006a,b; Sardi et al., 2006).

On the other hand, several studies have demonstrated a geographic structure in modern human craniometric diversity on a global level (e.g., Howells, 1973, 1989; Hanihara, 1996). Craniometric data have been found to follow a common geographic pattern with genetic markers, including both classical and microsatellite DNA markers (Relethford, 1994, 2004a, 2009; Manica et al., 2007; Betti et al., 2009). These findings have been interpreted as resulting from an isolation-by-distance model of evolutionary diversification. Furthermore, population relationships inferred from cranial morphology (as reflected both by traditional linear measurements and by 3D geometric morphometric data) have been shown to match those inferred from genetic data (Roseman, 2004; Harvati and Weaver, 2006a,b; Smith, 2009).

Taken together, these results suggest that human cranial morphology preserves a relatively strong population history signal, in addition to a climatic and possibly also dietary/masticatory signal (e.g., Relethford, 2004a). In view of the prevalence of cranial morphology in interpreting the human fossil record, however, it is imperative to elucidate the effects of these processes on the cranium and to determine as much as possible which anatomical regions or measurements reflect adaptive or developmental changes and which can be reliably used to reconstruct phylogeny. Here, we follow up on previous work on the climatic and population history signature in the morphological diversity of modern human population using a modern human craniometric dataset (Hanihara, 1996, 1997) several times larger than the Howells dataset (1973, 1989) and other datasets used in most previous analyses (e.g., Harvati and Weaver, 2006a,b; Smith, 2009). The goals of our study are as follows: 1) to explore this unique dataset for patterns of correlation with geography and climate such as those found in analyses of smaller datasets (e.g., Howells, 1996; Roseman, 2004; Harvati and Weaver, 2006a,b; Smith, 2009); 2) to determine which of the linear measurements analyzed present higher inter-regional diversity than would be expected due to purely stochastic microevolutionary processes; 3) whether these measurements are correlated to climatic variables; and finally 4) to identify the geographic regions responsible for the differentiation seen in each of these variables.

MATERIALS AND METHODS

Our sample comprises 7,422 male modern human crania representing 135 geographic populations. A list of the populations used, sample size, geographic coordinates, and climate parameters obtained for each is presented in the Appendix. Populations were selected from the larger dataset collected by one of us (TH) according to sample size: only samples larger than 15 individuals were included in the analysis. Females were excluded because far fewer population samples were measured for females relative to males, resulting in much smaller female total sample. In a few cases, closely related populations were pooled to maximize sample size (see Appendix for details). All crania were measured by one observer (TH) and each individual is represented in this study by 33 linear measurements (Table 1). For each population, geographic coordinates were established to the closest reference point possible and climatic variables were obtained from BIOCLIM database using the DIVA-GIS software (Hijmans et al., 2004). Climatic variables collected include temperature-related as well as humidity and rainfall measurements (Appendix).

Before analysis, size correction was performed by dividing each measurement by the geometric mean of the individual (Darroch and Mosimann, 1985). Missing values were replaced by multiple regression estimations. The estimated values in this case correspond to the expected value of the missing variable (used as the dependent variable in the multiple regression) based on the remaining observed variables of that individual (which are used as the independent parameters of the regression). One multiple regression is performed for every variable that has missing values in a dataset that has all missing values replaced by the global mean of

TABLE 1. Linear measurements included in this study

Variables	Reference
Maximum cranial length (GOL)[a]	Brauer, 1988
Nasion-opisthocranion (NOL)[a]	Brauer, 1988
Cranial base length (BNL)[a]	Brauer, 1988
Maximum cranial breadth (XCB)[a]	Brauer, 1988
Minimum frontal breadth (M9)[a]	Martin and Saller, 1957
Maximum frontal breadth (XFB)[a]	Brauer, 1988
Biauricular breadth (AUB)[a]	Brauer, 1988
Biasterionic breadth (ASB)[a]	Brauer, 1988
Basion–bregma height (BBH)[a]	Brauer, 1988
Sagittal frontal arc (M26)[a]	Martin and Saller, 1957
Saggital parietal arc (M27)[a]	Martin and Saller, 1957
Saggital occipital arc (M28)[a]	Martin and Saller, 1957
Nasion-bregma chord (FRC)[a]	Brauer, 1988
Bregma-lambda chord (PAC)[a]	Brauer, 1988
Lambda-opisthion chord (OCC)[a]	Brauer, 1988
Basion prosthion length (BPL)	Brauer, 1988
Breadth between frontomalare temporale (M43)	Martin and Saller, 1957
Bizygomatic breadth (ZYB)	Brauer, 1988
Nasion prosthion height (NPH)[b]	Brauer, 1988
Interorbital breadth (DKB)[b]	Brauer, 1988
Orbital breadth (M51)[b]	Martin and Saller, 1957
Orbital height (OBH)[b]	Brauer, 1988
Nasal breadth (NLB)[b]	Brauer, 1988
Nasal height (NLH)[b]	Brauer, 1988
Palate breadth (MAB)[b]	Brauer, 1988
Mastoid height (MDH)	Brauer, 1988
Mastoid width (MDB)	Brauer, 1988
Frontal chord (M43(1))[b]	Martin and Saller, 1957
Frontal subtense (No 43c)[b]	Bräuer, 1988
Simotic chord (WNB)[b]	Brauer, 1988
Simotic subtense (SIS)[b]	Brauer, 1988
Zygomaxillary chord (ZMB)[b]	Brauer, 1988
Zygomaxillary subtense (SSS)[b]	Brauer, 1988

[a]Variables included in the neurocranium analysis.
[b]Variables included in the facial analysis.

each variable and the predicted values are subsequently used to replace the missing one. This procedure is preferable to simple mean replacement because of its relatively limited effect on the observed variance of a variable and on the covariances among variables. Multiple regressions were performed in Statistica 7 (Statsoft Inc., 1984–2007).

To test for patterns of correlation among morphology, geography, and climate, we calculated morphological, geographic, and climate distance matrices among all 135 groups (see Relethford, 2004a; Harvati and Weaver, 2006a,b). Morphological distances were calculated as Mahalanobis squared distances (Mahalanobis, 1936), which represent the morphological distance among groups, scaled by the inverse of the pooled within-group covariance matrix. In order to test the findings of previous studies showing that different cranial regions preserve population history and climatic signatures differentially (Harvati and Weaver, 2006a,b; Smith, 2009), three morphological distance matrices were calculated: one for the whole skull, one considering only facial variables, and the last one considering only neurocranial variables (Table 1). As genetic data are not available for all the populations included in this study, we used geographic distances as a proxy for genetic relationships, assuming a pattern of diversification through isolation by distance in accordance with the findings of Relethford and others (e.g., Relethford, 2004a; Manica et al., 2007; Betti et al., 2009). Geographic distance consisted of the linear distance between groups in kilometers, using Cairo, Bangkok, Bering and Panamá as check-points to limit the distances to terrestrial routes; and climate matrices are simply the differences among series for each climate variable. Distance matrices were compared through Mantel Correlation tests (Mantel, 1967), using NTSYSpc, version 2.10t (Rohlf, 1986–2000).

Our second objective was to determine which linear measurements show greater inter-regional diversity than would be expected due to stochastic microevolutionary processes alone. For this purpose, we calculated minimum Fst estimates (Relethford and Blangero, 1990; Relethford, 1994) for the whole set of variables and for each variable independently, using the 135 populations as the units of analysis. Fst offers a measure of the amount of variation found between the units of analysis in relation to the total variation of the sample expected under neutral evolution (Relethford, 1994). In other words, Fst gives an estimate of the amount of the variation that is a result of the differences observed between units of analysis (e.g. groups, populations). As such, it allows the assessment of the general influence of the subdivision of the data into groups in the overall variance observed. The Fst estimate has been originally devised for genetic data; however, it can also be derived from phenotypic data such as craniometric dimensions (Relethford and Blangero, 1990; Relethford, 1994) when the variance matrix for these data is proportional to the variance matrix of the genetic information underlying the phenotypic trait. As heritability (i.e., proportionality between phenotypic and genetic data) of craniometric measurements is usually relatively high (Devor, 1987; Carson, 2006), Fst estimates of such data offers a good parameter to compare the apportionment of intergroup variation seen for craniometric variables. Fst values were calculated in Excel, through a Macro written in Visual Basic by André Strauss (Instituto de Biociências, Universidade de São Paulo, Brazil), who allowed its usage for this study. We chose to analyze individual variables, rather than Principal Components, because we consider their interpretation to be more straightforward. Following the work of Relethford (1994, 2002) and the suggestion of Roseman and Weaver (2004), we accepted an Fst value of 0.3 as the threshold of variability that can be accepted as the product of stochastic microevolutionary processes alone. All Fst estimates considered here were based on an equal heritability value of 0.55, following previous studies (Devor, 1987; Relethford, 1994; Roseman and Weaver, 2004). Heritability values are used to correct Fst estimates so that it better reflects the proportionality between the phenotypic and the genetic variance matrices, and would present better estimates of Fst for those traits were the true heritability is known. Although Carson (2006) and Martínez-Abadías et al. (2009) published individual heritability estimates (h^2) for some of the variables used here, the use of Carson's results for those variables found to have high Fst values with $h^2 = 0.55$ did not change significantly the results (data not shown). Since both these studies found most h^2 values to be smaller than the one considered here (0.55), Fst estimates using their values would be much higher than the ones presented here. Thus, an h^2 of 0.55 must be seen as a conservative value in this case.

As a next step, we correlated those variables with high Fst values with the climatic variables, to see if the high intergroup diversity observed in these measurements can be explained by some of the environmental factors considered here. Because of the large sample size in this study, a very conservative alpha of 0.001 was adopted and so the climate correlations found are also considered conservative.

For the last objective of identifying the geographic regions responsible for this differentiation, the 135 populations were grouped in 15 geographic regions (Table 2; Fig. 1). For each region, Fst estimates were calculated for the groups in it, to see if our subdivisions into regional groupings could be considered coherent units from the viewpoint of internal variability. We then performed a jackknife procedure, removing all populations of one region at a time and recalculated the Fst for

TABLE 2. List of geographic regions, number of populations included, and Fst estimates for each

Region	Number of populations	Fst ($h^2 = 0.55$)
Australia	4	0.0873
East Africa	4	0.0843
East Asia	8	0.1132
Mediterranean	12	0.0846
Melanesia	20	0.1262
North Africa	3	0.0368
North and Central America	14	0.0997
Northeast Asia	3	0.1042
North Europe	18	0.0673
Extreme North America	12	0.1681
Polynesia	6	0.084
South Africa	4	0.0638
South America	4	0.0873
South Asia	17	0.101
West Africa	6	0.0486
Total	135	0.1467

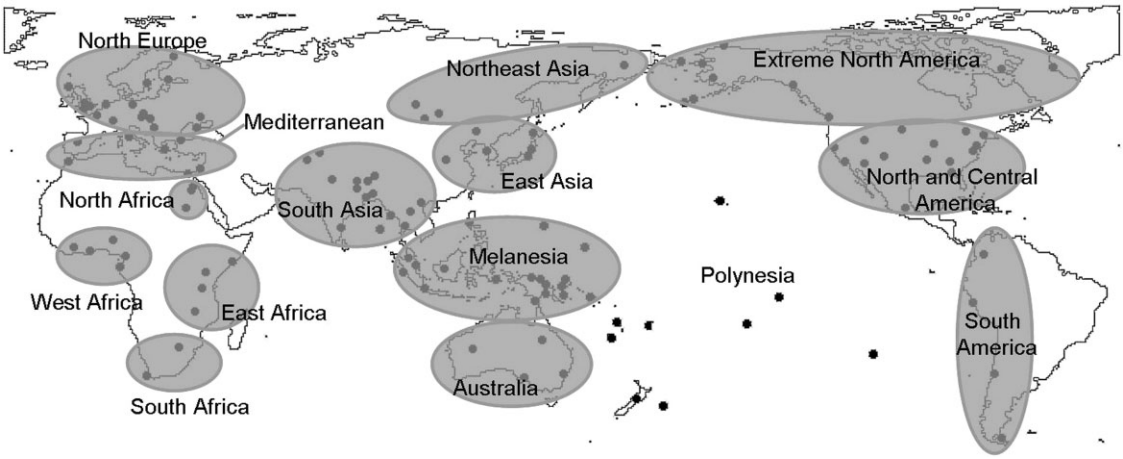

Fig. 1. Geographic regions in which the series included in the study were grouped. Polynesia includes all dark dots of the Pacific Ocean not included in a gray ellipsis.

TABLE 3. Mantel correlations results between morphological distances and geographic and climate distances

	Anatomical region		
Geographic and climate variables	Whole skull	Neurocranium	Face
Geographical distance	r = 0.3769 p = 0.0001	r = 0.4033 p = 0.0001	r = 0.2925 p = 0.0001
Temperature			
Annual minimum temperature	r = 0.3509 p = 0.0001	r = 0.2502 p = 0.0001	r = 0.3736 p = 0.0001
Annual maximum temperature	r = 0.3943 p = 0.0001	r = 0.3099 p = 0.0001	r = 0.3938 p = 0.0001
Annual average temperature	r = 0.3863 p = 0.0001	r = 0.2917 p = 0.0001	r = 0.3957 p = 0.0001
Maximum temperature of the warmest month	r = 0.2738 p = 0.0001	r = 0.2549 p = 0.0001	r = 0.2573 p = 0.0001
Minimum temperature of the coldest month	r = 0.3083 p = 0.0001	r = 0.1967 p = 0.0001	r = 0.3421 p = 0.0001
Temperature range	r = 0.1466 p = 0.0002	r = 0.0764 p = 0.0245	r = 0.1830 p = 0.0001
Precipitation			
Annual rainfall	r = −0.0142 p = 0.4125	r = −0.0211 p = 0.3613	r = −0. 436 p = 0.1323
Rainfall of the wettest month	r = 0.0117 p = 0.3636	r = −0.0295 p = 0.2404	r = 0.0149 p = 0.3176
Rainfall of the driest month	r = −0.0155 p = 0.4196	r = 0.0161 p = 0.6471	r = −0.0890 p = 0.0085
Relative humidity[a]	r = −0.0174 p = 0.3856	r = 0.0180 p = 0.3321	r = −0.0186 p = 0.3485

[a]Relative humidity correlations are based on 132 populations, since data for some Polynesian islands could not be retrieved.

those variables with values above the 0.3 threshold. This procedure allowed us to evaluate the effect of each region in the apportionment of between-group variation.

RESULTS

Geographic and Climate Correlations

The results of the Mantel correlations tests comparing morphological distances with geographic and climate variables (Table 3) support previous findings (Harvati and Weaver, 2006a,b; Smith, 2009) that, when considered as a whole, cranial morphology shows a strong correlation with geographic distance (r = 0.38; P = 0.0001). Significant correlations were also observed with some climate variables, especially those reflecting temperature (r ranging from 0.27 to 0.39, all significant at the 0.0001 level). When only neurocranial and only facial measurements were considered, the former showed a higher correlation coefficient with geographic distances (r = 0.40) and a lower one with temperature variables (r from 0.20 to 0.31), while the latter showed the inverse pattern (r = 0.29 for geography and ranging from 0.25 to 0.40 for climate; Table 3).

TABLE 4. Fst estimates for the variables included in the study

Variables	Fst ($h^2 = 0.55$)	Fst ($h^2 = 1.00$)
All Variables	0.2117	0.1287
Maximum cranial length (GOL)	0.2771	0.1741
Nasion-opisthocranion (NOL)	0.2843	0.1793
Cranial base length (BNL)	0.2335	0.1435
Maximum cranial breadth (XCB)	**0.4378**	0.2999
Minimum frontal breadth (M9)	0.1801	0.1078
Maximum frontal breadth (XFB)	**0.3812**	0.2531
Biauricular breadth (AUB)	**0.4934**	**0.3488**
Biasterionic breadth (ASB)	0.2730	0.1712
Basion –bregma height (BBH)	0.2765	0.1737
Sagittal frontal arc (M26)	0.1820	0.1090
Saggital parietal arc (M27)	0.1975	0.1172
Saggital occipital arc (M28)	0.1464	0.0862
Nasion-bregma chord (FRC)	0.1582	0.0937
Bregma-lambda chord (PAC)	0.2221	0.1357
Lambda-opisthion chord (OCC)	0.1494	0.0881
Basion prosthion length (BPL)	**0.3192**	0.2050
Breadth between Frontomalare temporale (M43)	0.2832	0.1785
Bizygomatic breadth (ZYB)	**0.4368**	0.2990
Nasion prosthion height (NPH)	**0.4017**	0.2697
Interorbital breadth (DKB)	0.2517	0.1599
Orbital breadth (M51)	0.2653	0.1657
Orbital height (OBH)	0.2801	0.1703
Nasal breadth (NLB)	**0.3500**	0.2285
Nasal height (NLH)	**0.3636**	0.2391
Palate breadth (MAB)	0.2365	0.1456
Mastoid height (MDH)	0.2038	0.1234
Mastoid width (MDB)	0.1830	0.1097
Frontal chord (M43(1))	0.2363	0.1454
Frontal subtense (No 43c)	0.2775	0.1744
Simotic chord (WNB)	0.2657	0.1660
Simotic subtense (SIS)	**0.3481**	0.2270
Zygomaxillary chord (ZMB)	**0.3608**	0.2369
Zygomaxillary subtense (SSS)	0.2508	0.1555

Variables with Fst estimates higher than 0.3 are shown in bold.

Apportionment of the Variation of Craniometric Dimensions

Table 4 lists the Fst values calculated for the entire set of craniometric measurements and for each of the variables separately. The value obtained (0.21 for $h^2 = 0.55$) for all measurements considered together, representing overall cranial morphology, is similar (if a little higher) to Fst values published previously for cranial morphology at a worldwide level (Relethford, 1994, 2002). This result shows that increasing the number of population samples, as well as the total number of specimens considered in the analysis, does not affect the observed pattern of apportionment of craniometric variation. Of the Fst values calculated for each measurement separately, 10 of the 33 were relatively high (>0.3). The variables with high Fst values are concentrated in the facial region, and reflect facial height (NPH), breadth (ZYB, ZMB) and projection (BPL), and the dimensions of the nasal aperture (NLB, NLH, and SIS). Only three neurocranial measurements showed high Fst values, and all reflect cranial breadth (XCB, XFB, and AUB). From these variables, those associated with cranial breadth and with nasal height have previously been correlated with temperature by Roseman (2004) and thus suggested to be influenced by selection to cold climatic conditions.

Climate Correlations of Variables with High Amounts of Intergroup Variation

The correlation coefficients and probability values obtained between the cranial measurements with high Fst values and the climate variables compiled for this study are reported in Table 5. The strongest relationship was found with temperature variables, which were strongly correlated with (in order of greatest r) facial height (NPH; r ranging from −0.57 to −0.71), nasal height (NLH; r ranging from −0.53 to −0.64) and biauricular breadth (AUB; r ranging from −0.55 to −0.65), as well as with facial breath (ZYB; r ranging from −0.45 to −0.56), nasal breadth (NLB; r ranging from −0.38 to −0.48), and the other two neurocranial breadth measurements (XCB, XFB; r ranging from −0.38 to −0.47 and from −0.33 to −0.41, respectively). Relative humidity was also correlated with breadth dimensions, both in the face (ZYB; r = 0.40) and in the neurocranium (XCB and AUB; r = 0.33 and 0.38, respectively). Finally, precipitation and temperature range appear correlated to nasal breadth, as well as, more weakly, to some of the other dimensions, mostly in the face (BPL, NPH, NLB, and SIS for precipitation; BPL, NPH, NLH, and AUB for temperature range). The only variable with high Fst which does not show a significant correlation with climate variables was one reflecting mid-facial breadth (ZMB).

TABLE 5. Correlations coefficients and associated probabilities between the variables with high Fst values and the climate parameters included in this study

Craniometric variables	Temperature						Precipitation			
	Annual minimum temperature	Annual maximum temperature	Annual average temperature	Maximum temperature of warmest month	Minimum temperature of coldest month	Temperature range	Annual Rainfall	Rainfall of wettest month	Rainfall of driest month	Relative humidity
XCB	**−0.4037**	**−0.4662**	**−0.4421**	**−0.3966**	**−0.3782**	0.2109	−0.1353	−0.1156	−0.1214	**0.3302**
	$p < 0.001$	$p < 0.001$	$p < 0.001$	$p < 0.001$	$p < 0.001$	$p = 0.015$	$p = 0.122$	$p = 0.187$	$p = 0.166$	$p < 0.001$
XFB	**−0.3634**	**−0.4097**	**−0.3930**	**−0.3281**	**−0.3473**	0.2170	−0.2188	−0.1637	−0.2363	0.2593
	$p < 0.001$	$p < 0.001$	$p < 0.001$	$p < 0.001$	$p < 0.001$	$p = 0.012$	$p = 0.012$	$p = 0.061$	$p = 0.006$	$p = 0.003$
AUB	**−0.5862**	**−0.6459**	**−0.6253**	**−0.5720**	**−0.5458**	**0.3046**	−0.1136	−0.1332	−0.0154	**0.3766**
	$p < 0.001$	$p < 0.001$	$p < 0.001$	$p < 0.001$	$p < 0.001$	$p < 0.001$	$p = 0.195$	$p = 0.128$	$p = 0.861$	$p < 0.001$
BPL	0.1403	0.0863	0.1144	−0.0971	0.1889	**−0.2957**	**0.3252**	**0.3022**	**0.2650**	0.1401
	$p = 0.109$	$p = 0.325$	$p = 0.192$	$p = 0.268$	$p = 0.030$	$p < 0.001$	$p < 0.001$	$p < 0.001$	$p = 0.002$	$p = 0.109$
ZYB	**−0.4953**	**−0.5623**	**−0.5367**	**−0.5461**	**−0.4460**	0.1982	0.0126	−0.0190	0.0805	**0.4018**
	$p < 0.001$	$p < 0.001$	$p < 0.001$	$p < 0.001$	$p < 0.001$	$p = 0.023$	$p = 0.886$	$p = 0.829$	$p = 0.359$	$p < 0.001$
NPH	**−0.7022**	**−0.7021**	**−0.7117**	**−0.5695**	**−0.6759**	**0.4668**	−0.2697	**−0.2919**	−0.1169	0.2151
	$p < 0.001$	$p < 0.001$	$p < 0.001$	$p < 0.001$	$p < 0.001$	$p < 0.001$	$p = 0.002$	$p = 0.001$	$p = 0.182$	$p = 0.013$
NLB	**0.4377**	**0.4791**	**0.4655**	**0.3832**	**0.3863**	−0.2296	**0.3176**	**0.4501**	0.0797	−0.1553
	$p < 0.001$	$p < 0.001$	$p < 0.001$	$p < 0.001$	$p < 0.001$	$p = 0.008$	$p < 0.001$	$p < 0.001$	$p = 0.364$	$p = 0.075$
NLH	**−0.6016**	**−0.6365**	**−0.6278**	**−0.5342**	**−0.5885**	**0.3817**	−0.0996	−0.1187	0.0092	0.2566
	$p < 0.001$	$p < 0.001$	$p < 0.001$	$p < 0.001$	$p < 0.001$	$p < 0.001$	$p = 0.256$	$p = 0.175$	$p = 0.917$	$p = 0.003$
SIS	−0.0357	0.0022	−0.0168	0.1347	−0.0452	0.1426	**−0.3057**	**−0.3997**	−0.1167	−0.2076
	$p = 0.685$	$p = 0.980$	$p = 0.848$	$p = 0.124$	$p = 0.607$	$p = 0.103$	$p < 0.001$	$p < 0.001$	$p = 0.183$	$p = 0.017$
ZMB	−0.1555	−0.1618	−0.1606	−0.1938	−0.1532	0.0641	0.1844	0.2618	0.0603	0.2077
	$p = 0.075$	$p = 0.064$	$p = 0.066$	$p = 0.026$	$p = 0.079$	$p = 0.466$	$p = 0.034$	$p = 0.002$	$p = 0.492$	$p = 0.017$

Significant correlation at $\alpha = 0.001$ are shown in bold.

Influence of Each Region on the Apportionment of Variation

With the exception of Extreme North America, all regions showed fairly low Fsts (Table 2), lower than the Fst estimate obtained for the entire dataset, justifying the geographic criteria adopted for the grouping of the populations into regions. The high Fst found for Extreme North America may be due to the large geographic distances observed among the samples it included. However, it was kept as a region due to the impossibility of further subdivision.

Figure 2 shows the results of the jackknifing procedure of the regions in calculating Fsts values for each of the 10 variables with a high proportion of intergroup variation (i.e., the variables listed in bold in Table 4). The columns depicted in the figure present the value of Fst obtained after removing the geographic region indicated under each column, as well as the Fst obtained originally with all groups included. To facilitate the reading of the graphs, the Fst values have been sorted in increasing order. As a way to assess the significance of the values obtained after removing each region, the graphs also show in darker gray those values that fall bellow the 95% confidence range of the original Fst. The confidence limit in this case was calculated as the value of the Fst for all region −1.96 times the standard deviation of the Fst values obtained with the jackknifing procedure. As can be observed, in all cases at least the lowest Fst value obtained is below this confidence limit. In no case was the highest Fst obtained in these analyses above the 95% confidence limit (original Fst + 1.96 times the standard deviation). This suggests that the reduction in Fst observed is more accentuated than its increase.

The pattern that emerges from these analyses regards the impact of the northernmost regions on the Fst values of these measurements. As can be observed, for eight of the variables, the regions that contribute most for the intergroup diversification (i.e., the regions that by being removed reduce the Fst values most) are the northernmost (Northern Europe, Northeast Asia, or Extreme North America). However, while the removal of Northeast Asia and Extreme North America always appear to affect the Fst of the same variables, the removal of Northern Europe mostly affects the Fst of different measurements. Since Northeast Asia and Extreme North America behave in a similar manner, the effect of their removal together is also plotted in Fig. 2. These two regions contribute most to the intergroup differentiation seen in facial and nasal height (NPH, NLH), facial breadth (ZYG), and biauricular breadth (AUB), (Fig. 2f,h,c,d, respectively). The removal of Northern Europe, on the other hand, affected most the Fst values for frontal breadth (XFB), facial projection (BPL), and nasal breadth (NLB; Fig. 1b,e,g, respectively). These three geographic regions together also affected the Fst observed for midfacial breadth (ZMB; Fig. 1j), the only variable that did not show a strong correlation with the climate parameters included in this study.

The two remaining variables (XCB and SIS) show a strong contribution of regions other than the three northernmost. Maximum cranial breadth is mostly influenced by Australia and Melanesia (although only this first is below the 95% confidence range) and simotic chord is influenced mostly by South Africa and North Europe (both below the 95% confidence range).

To summarize, the jackknife analyses performed suggest that most of the variables with a high amount of

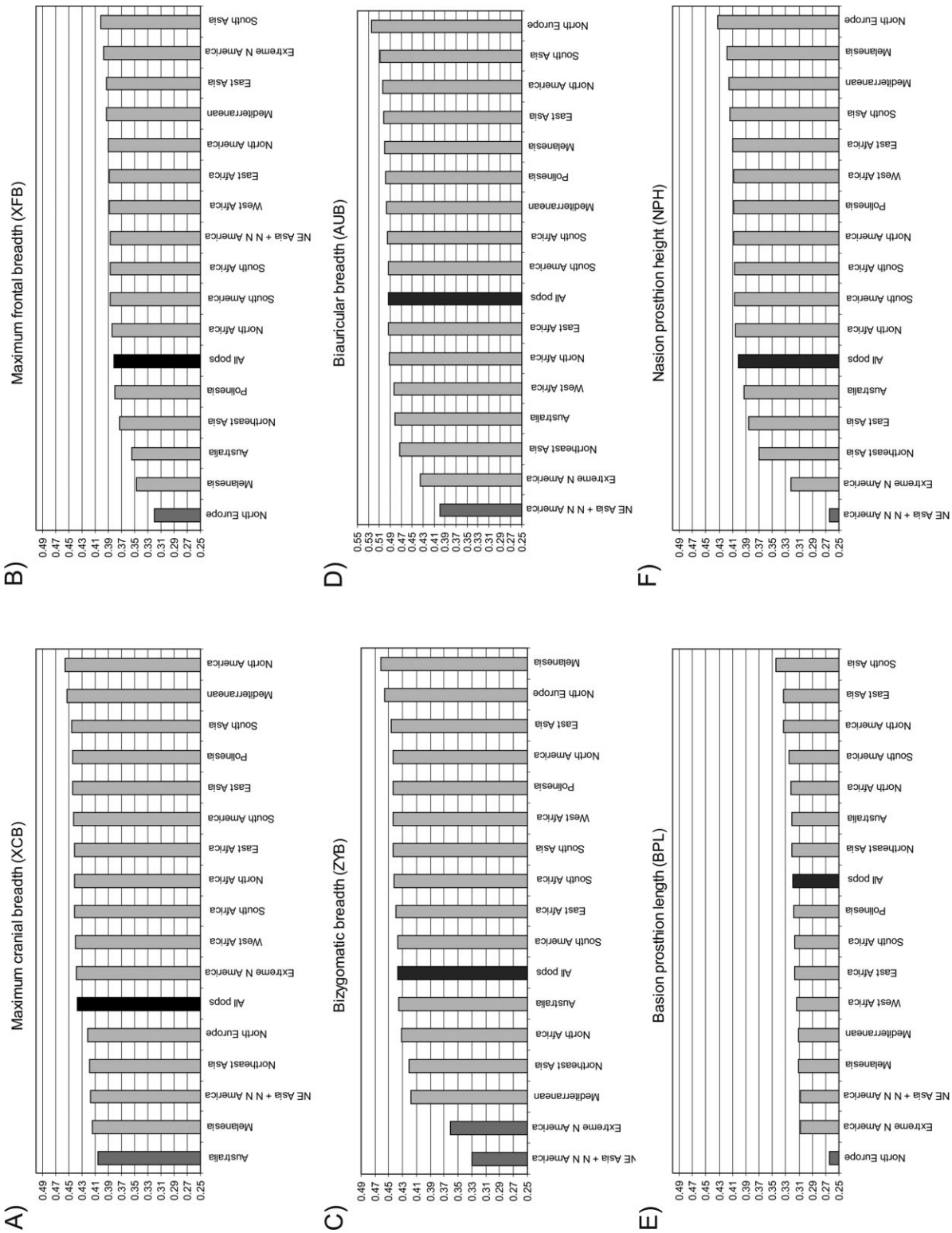

Fig. 2. Effects of the removal of each of the geographic regions in the Fst estimates of the variables presenting high between-group variation apportionment (Fst $>$ 0.3). The black columns show the Fst obtained with all regions included. Dark gray columns represent those regions whose Fst value falls bellow the 95% confidence of the jackknife procedures (refer to text for more details).

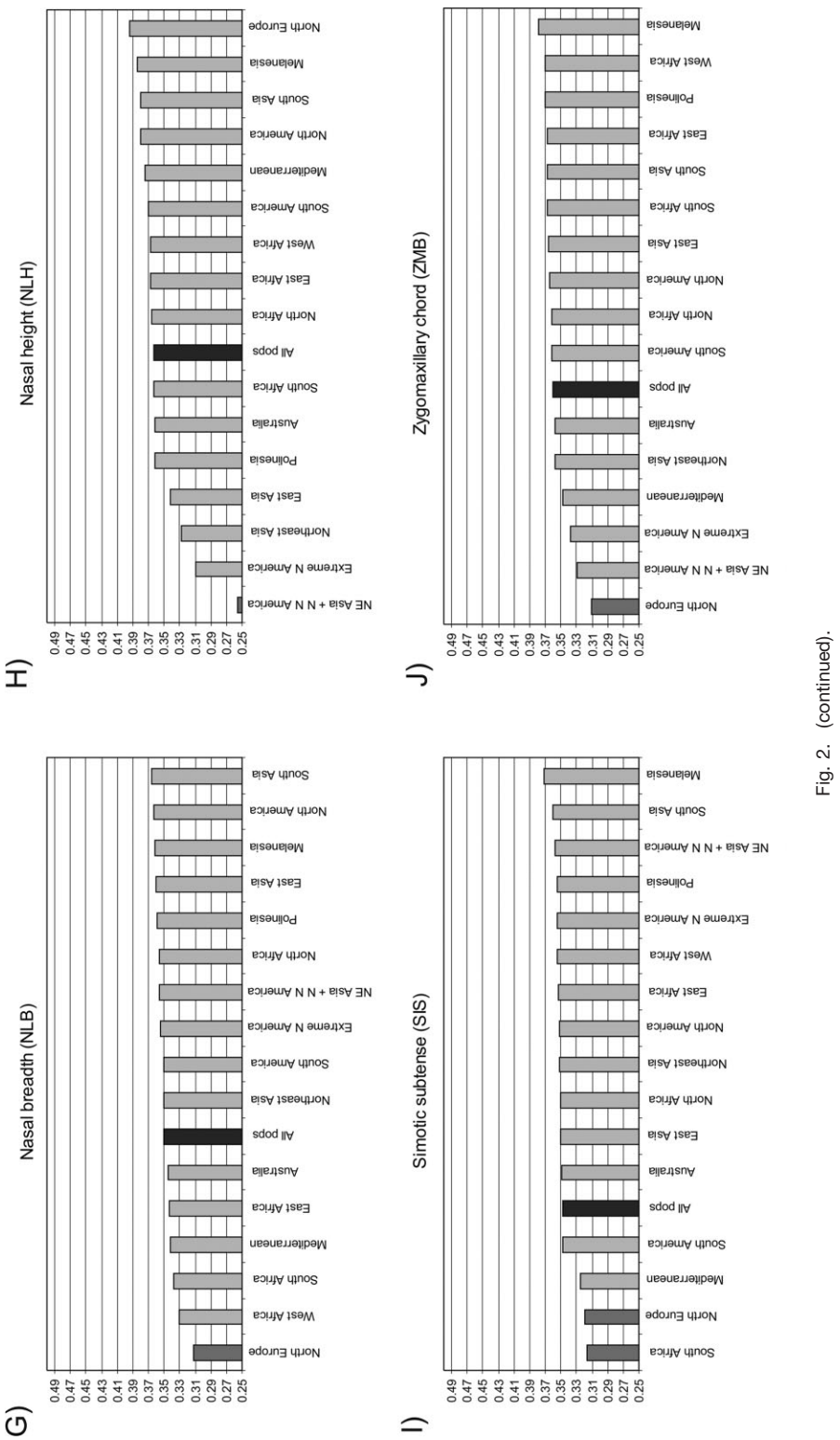

Fig. 2. (continued).

intergroup variation which are strongly correlated with climate variables have a significant part of their differentiation driven by populations living in the northernmost regions of the planet. Also, it appears that morphological differentiation of these northernmost populations was not uniform, because the measurements under the influence of Northern Europe are a distinct set from those influenced by Northeast Asia and Extreme North America.

DISCUSSION

The results presented here indicate a strong relationship between cranial morphology and geographic distance, similar to that found by Relethford (2004a) in a much smaller population and total sample. Our findings further suggest a climatic signature on the morphological diversity of modern human groups, evidenced by both the morphological distances among group centroids and by the apportionment of between-group variation. Our study agrees well with previous work on limited geographic and total samples indicating that both isolation by distance and climate adaptation explain cranial morphological variation in modern humans (Relethford, 2004b; Roseman 2004; Harvati and Weaver, 2006a,b; Smith, 2009).

Our results also confirm that different anatomical regions are affected differentially by population history, here assumed to be closely related to geographic distance, and by environmental conditions, as previously suggested (Roseman, 2004, Harvati and Weaver, 2006; Smith, 2009). Although the nature of the linear measurements we used here did not allow as fine a subdivision of the cranium as is possible with geometric morphometric data (see Harvati and Weaver, 2006a,b; Smith, 2009), we were able to partition our data into neurocranial and facial measurements, and to consider these in our analysis in addition to the complete cranial dataset. We found that, while a larger part of neurocranial variability can be explained by geographic, rather than climatic, distances, facial morphology exhibits the opposite pattern. If geographic distances can be used as a proxy to genetic distances and population history in situations where isolation by distance is an important microevolutionary force, as has been suggested for modern humans (Relethford, 2004b), this result implies that neurocranial variability reflects population history to a greater degree than climate, in agreement with Harvati and Weaver (2006a,b; but contra Smith, 2009). Nonetheless, the facial measurements in the present study were found to be correlated, albeit more weakly than neurocranial measurements, with geographic distances as well as with climate. This result supports the recent finding by Smith (2009), who reported that facial morphology was correlated with neutral genetic distances (contra Harvati and Weaver, 2006b).

In agreement with these findings, our Fst analysis of individual measurements suggests that roughly one third of the craniofacial measurements studied are associated with higher Fst values than would be expected as result of stochastic microevolutionary forces alone. Most of these variables are concentrated on the face and are correlated with some aspects of climate. However, the high Fst values observed in these variables were mostly influenced by populations living in the northernmost regions of the planet, i.e., extreme North America, Northeast Asia, and Northern Europe. This result agrees with previous studies that found no correlation between climate and cranial morphology once Arctic samples were removed from the analyses and that suggested that climatic adaptation was observed in populations living under extreme cold conditions (Roseman, 2004; Harvati and Weaver, 2006b).

Most of the high Fst variables showing a correlation with climate were located on the face, with a few also reflecting neurocranial breadth, again agreeing with previous work (Coon et al., 1950; Carey and Steegmann, 1981; Beals et al., 1983; Franciscus and Long, 1991; Roseman, 2004; Roseman and Weaver, 2004; Harvati and Weaver, 2006a,b). They comprise measurements of facial breadth and height, as well as the nasal dimensions and simotic subtense. The cranial breadth measurements, facial height and breadth, and nasal dimensions were correlated with temperature variables; while nasal breadth and, to a lesser extent, nasal height, simotic subtense, and facial projection were correlated with rainfall variables. Two of the three cranial breadth measurements and facial breadth were correlated with relative humidity. These measurements were also found by Roseman (2004) to be related to climate.

The results of the jackknife procedure of the regions suggest that, although the northernmost populations are those that are maximally affecting the Fst values of the variables with high degrees of interpopulation variability, these regions influence different sets of measurements, and therefore different aspects of cranial morphology. While Northeast Asia and extreme North America affect mostly facial height and breadth, nasal height and inferior cranial breadth, Northern European populations influence facial projection, nasal breadth, and frontal breadth. These results suggest that populations from these regions followed distinct adaptive pathways to their cold environment. These different pathways are evident in two sets of variables: the nasal dimensions and the neurocranium breadth. In all three extreme cold regions included here, adaptation to cold climate in nasal shape seems to have favored small breadth/height relations of the nasal cavity: extreme North America, Northeast Asia, and Northern Europe show the lowest nasal index of all 15 regions. Yet, the path by which small nasal indexes have been achieved is different for each region. While Northern Europe populations exhibit the smallest mean nasal breadth, Northeast Asia and extreme North America show the largest mean nasal height. Both strategies result in smaller nasal indexes. The same pattern is observed for the facial height, which suggests that this measure might be reflecting the nasal height that is included in it.

Similarly, when cranial breadth is considered, all three northernmost regions (together with East Asian series) are characterized by wide neurocrania, although the regional differentiation is associated with distinct measurements: while Northern European groups are mainly affecting the Fst of maximum frontal breadth, Northeast Asians and Extreme North Americans are affecting the Fst observed for biauricular breadth. These differences can be interpreted again as distinct pathways toward wider braincases, which would be advantageous for populations in extremely cold climates under the assumption of Bergman's and Allen's rules (Beals et al., 1983, 1984): By increasing neurocranium breadth, globularity of the braincase is increased and the ratio surface/volume reduced, thus reducing heat loss through the surface of the skull. These changes toward a wider skull could be related to changes in basicranial morphology, which seems to be influencing vault morphology (Lieberman et al., 2000), as

well as to the increase of general brain size (Beals et al., 1984). However, the lack of basicranial measurements in our dataset limits at this moment our capacity to further explore these hypotheses.

The distinct adaptive pathways suggested here could be the result of the constraints on the morphology of each population derived from its unique population history; or, alternatively, as a result of differences in the complex interplay among the various climatic parameters (e.g., temperature, humidity, rainfall, seasonality, etc.), only some of which could be included in this study. It is also possible that some of the measurements with greater-than-expected Fst values, particularly those on the face, are additionally influenced by other types of adaptation, most importantly related to dietary or masticatory practices. While dietary factors were not included in our study, the extreme masticatory and paramasticatory behavior of some extreme North American populations is well documented (e.g., Applet et al., 2000), and could be contributing to the observed pattern of high population diversity. This could be particularly relevant for those variables related to the masticatory complex, such as bi-zygomatic breadth, which is influenced by the size of the masticatory muscles (temporalis and masseter).

Our results also have some implications for the interpretation of the Neanderthal distinctive morphology, which has in the past been interpreted as resulting from climatic adaptation (e.g., Coon et al., 1950; Sergi, 1958). However, it has been observed that Neanderthal facial and especially nasal morphology does not necessarily match expected climatic patterns seen among modern human populations, and is sometimes described as a "paradox" (e.g., Holton and Franciscus, 2008; though see Márquez and Laitman, 2008 for an example of wide nasal apertures in cold climates in macaques). Alternative explanations for the evolution of the Neanderthal face have focused on functional demands associated with paramasticatory activities (e.g., Rak, 1986; Trinkaus, 1987) or on random genetic drift (e.g., Howell, 1952; Hublin, 1998) as driving forces. A recent study by Weaver et al. (2007) could not reject genetic drift as responsible for the evolution of Neanderthal cranial morphology, though selection was not excluded particularly for some aspects of facial anatomy. Here we have shown that different cold-adapted modern human populations do not show identical morphological patterns in response to their environments. Instead they appear to have followed distinct trajectories probably constrained by their ancestral morphology as well as by subtle differences in their environments. In this context, one might expect a possible Neanderthal cold adaptation to share some elements with the observed pattern in modern humans, but to be limited by the ancestral morphology of that species. Given the constrains of such morphology (i.e., elongated, low crania, tall faces, wide nasal apertures), the greatly increased height of the Neanderthal nasal aperture, as well as their increased cranial breadth, relative to the ancestral morphology are consistent with an adaptation to extremely cold climates.

Finally, since our assessment of climate signature in the morphological differentiation of modern human population is based mostly on Fst estimation for individual craniometric measurements, some notes of caution are in order. First, the fact that we chose to consider as significant only those variables with Fst values higher than 0.3 means that our conclusions are centered on diversifying evolutionary forces. As stated by Roseman (2004) and Roseman and Weaver (2004), stabilizing selection could also be affecting general morphological trends in modern humans. Such stabilizing selection would result in a reduction of Fst estimates for those variables or anatomical regions affected. However, no apparent reduction of Fst estimates was observed in our analysis. The variable with smallest Fst estimate (Occipital arc; Fst = 0.1464) is relatively close to the Fst estimate for the whole cranium (0.2117), and well within the range of Fst estimates published for neutral molecular data (Lewontin, 1972) and other craniometric datasets (Relethford, 1994, 2002).

Second, Fst estimates for craniometric traits depend a great deal on reliable estimates of heritability (Relethford and Blangero, 1990; Relethford, 1994). Carson (2006) and Martínez-Abadías et al. (2009) presented estimates for heritability of craniometric measurements that are in most cases smaller than the usually accepted heritability values of 0.55 (Devor, 1987; Sparks and Jantz, 2002). The consequence of assuming a moderately high and uniform heritability means that we are probably underestimating the number of variables that have real Fst values above the threshold of 0.3. Thus, although the heritability value assumed here does not affect the variables presented as having high degrees of between population diversity, it probably excluded a number of variables that would have been included in this category, had we used the more recent heritability estimates.

In conclusion, both geographic distances and climate differences seem to contribute to the morphological diversity seen among modern human populations. Assuming that geographic distances reflect isolation by distance processes of morphological differentiation due to stochastic microevolutionary forces (Relethford, 2004a; Harvati and Weaver, 2006a,b) and that climate signature might be a result of diversifying selection (Relethford, 2004b; Roseman, 2004; Harvati and Weaver, 2006a,b), our analysis corroborates that the between-groups cranial morphological variation has been shaped both by neutral evolutionary processes and natural selection.

Diversifying selection to cold environments mainly affects dimensions in the face and neurocranial breadth. High Fst values, pointing to diversifying selection, are apparent in the northernmost populations of Europe, Asia, and America. This pattern has been previously observed for North American groups (Roseman, 2004; Harvati and Weaver, 2006b) in much smaller samples (10–13 geographic population samples, comprising one Arctic sample each). Although natural selection to cold climate seems to have been a considerable force of morphological differentiation among modern humans, it appears limited to northern populations and has not eliminated the geographic, population history, signal observed in the overall pattern of modern human craniometric differentiation. Furthermore, diversifying selection to similar environmental conditions was found here to follow distinct pathways of morphological differentiation among the northern populations of Europe, East Asia, and North America. Some aspects of Neanderthal morphology are consistent with an adaptation to extreme cold conditions, given the constraints of their ancestral morphology.

ACKNOWLEDGMENTS

The authors thank Danilo Vicensotto Bernardo for his help with the original database, and André Strauss for sharing with us his Visual Basic code which allowed us to perform

the Fst calculations. Two anonymous reviewers provided helpful comments, which improved this manuscript.

LITERATURE CITED

Applet M, Berglund J, Gullov HC. 2000. Identities and cultural contacts in the Arctic. Copenhagen: Danish Polar Center.

Beals KL, Smith CL, Dodd SM. 1983. Climate and the evolution of brachycephalization. Am J Phys Anthropol 62:425–437.

Beals KL, Smith CL, Dodd SM. 1984. Brain size, cranial morphology, climate and time machines. Curr Anthropol 25:301–330.

Betti L, Balloux F, Amos W, Hanihara T, Manica AL. 2009. Distance from Africa, not climate, explains within-population phenotypic diversity in humans. Proc R Soc B 276:809–814.

Carey JW, Steegmann AT. 1981. Human nasal protrusion, latitude, and climate. Am J Phys Anthropol 56:313–319.

Carson EA. Maximum likelihood estimation of human craniometric heritabilities. Am J Phys Anthropol 131:169–180.

Collard M, Wood B. 2000. How reliable are human phylogenetic hypotheses? Proc Natl Acad Sci USA 97:5003–5006.

Coon CS, Garn SM, Birdsell JB. 1950. Races: a study of the problems of race formation in man. Springfield: Charles C. Thomas.

Darroch JN, Mosimann JE. 1985. Canonical and principal components of shape. Biometrika 72:241–252.

Devor EJ. 1987. Transmission of human craniofacial dimensions. J Craniofac Genet Dev Biol 7:95–106.

Franciscus RG, Long JC. 1991. Variation in human nasal height and breadth. Am J Phys Anthropol 85:419–427.

González-José R, Ramírez-Rozzi F, Sardi M, Martínez-Abadías N, Hernández M, Pucciarelli HM. 2005. A functional-cranial approach to the influence of economic strategy on skull morphology. Am J Phys Anthropol 128:757–771.

Hanihara T. 1996. Comparison of craniofacial features of major human groups. Am J Phys Anthropol 99:389–412.

Hanihara T. 1997. Craniofacial affinities of Mariana Islanders and Circum-Pacific peoples. Am J Phys Anthropol 104:411–425.

Harvati K. 2003. Quantitative analysis of Neanderthal temporal bone morphology using 3-D geometric morphometrics. Am J Phys Anthropol 120:323–338.

Harvati K, Hubbe M, Bernardo DV, Hanihara T. 2009. Population history and cranial morphology in a large human skeletal dataset. Am J Phys Anthropol S48:145–146.

Harvati K, Weaver TD. 2006a. Reliability of cranial morphology in reconstructing Neanderthal phylogeny. In: Harvati K, Harrison T, editors. Neanderthals revisited: new approaches and perspectives. New York: Springer.

Harvati K, Weaver T. 2006b. Human cranial anatomy and the differential preservation of population history and climate signatures. Anat Rec 288A:1225–1233.

Hijmans RJ, Guarino L, Jarvis A, O'Brien R, Mathur P. 2004. DIVA-GIS Version 5.2.0.2. Available at: http://www.diva-gis.org.

Holton NE, Franciscus RG. 2008. The paradox of a wide nasal aperture in cold-adapted Neandertals: a causal assessment. J Hum Evol 55:942–951.

Howell FC. 1952. Pleistocene glacial ecology and the evolution of "classic" Neandertal man. Southwest J Anthropol 8:377–410.

Howells WW. 1973. Cranial variation in man: a study by multivariate analysis of patterns of difference among recent human populations. Cambridge: Harvard University.

Howells WW. 1989. Skull shapes and the map: craniometric analyses in the dispersion of modern Homo. Cambridge: Harvard University.

Howells WW. 1996. Howells' craniometric data on the internet. Am J Phys Anthropol 101:441–442.

Hublin J-J. 1998. Climatic changes, paleogeography, and the evolution of the Neandertals. In: Akazawa T, Aoki K, Bar-Yosef O, editors. Neandertals and modern humans in Western Asia. New York: Plenum Press. p 295–310.

Hylander WL. 1977. The adaptive significance of Eskimo craniofacial morphology. In: Dahlberg AA, Graber TM, editors. Orofacial growth and development. Chicago: Mouton. p 129–170.

Larsen CS. 1999. Bioarchaeology: interpreting behavior from the human skeleton. Cambridge: Cambridge University Press.

Lewontin R. 1972. The apportionment of human diversity. In: Hecht M, Steere W, editors. Evolutionary biology. New York: Plenum. Vol 6, p 381–398.

Lieberman DE, Krovitz GE, Yates FW, Devlin M, St. Claire M. 2004. Effects of food processing on masticatory strain and craniofacial growth in a retrognathic face. J Hum Evol 46:655–677.

Lieberman DE, Pearson OM, Mowbray KM. 2000. Basicranial influence on overall cranial shape. J Hum Evol 38:291–315.

Mahalanobis PC 1936. On the generalized distance in statistics. Proc Natl Inst Sci India 2:49–55.

Manica A, Amos W, Balloux F, Hanihara T. 2007. The effect of ancient population bottlenecks on human phenotypic variation. Nature 448:346–348.

Mantel N. 1967. The detection of disease clustering and a generalized regression approach. Cancer Res 27:209–220.

Márquez S, Laitman J. 2008. Climatic effects on the nasal complex: a CT imaging, comparative anatomical, and morphometric investigation of *Macaca mulatta* and *Macaca fascicularis*. Anat Rec 291:1420–1445.

Martin R, Saller K. 1957. Lehrbuch der Anthropologie. Stuttgart: Gustav Fischer Verlag.

Martínez-Abadías N, Esparza M, Sjøvold T, González-José R, Santos M, Hernández M. 2009. Heritability of human cranial dimensions: comparing the evolvability of different cranium regions. J Anat 214:19–35.

Olson TR. 1981. Basicrania and evolution of the Pliocene hominids. In: Stringer CB, editor. Aspects of human evolution. London: Taylor and Francis. p 99–128.

Rak Y. 1986. The Neanderthal: a new look at an old face. J Hum Evol 15:151–164.

Relethford JH. 2002. Apportionment of global human genetic diversity based on craniometrics and skin color. Am J Phys Anthropol 118:393–398.

Relethford JH. 1994. Craniometric variation among modern human populations. Am J Phys Anthropol 95:53–62.

Relethford JH. 2004a. Boas and beyond: migration and craniometric variation. Am J Hum Biol 16:379–386.

Relethford JH. 2004b. Global patterns of isolation by distance based on genetic and morphological data. Hum Biol 76:499–513.

Relethford JH. 2009. Race and global patterns of phenotypic variation. Am J Phys Anthropol 139:16–22.

Relethford JH, Blangero J. 1990. Detection of differential gene flow from patterns of quantitative variation. Hum Biol 62:5–25.

Relethford JH, Crawford MH, Blangero J. 1997. Genetic drift and gene flow in post-famine Ireland. Hum Biol 69:443–465.

Rohlf FJ. 1986–2000. Copyright. NTSYSpc version 2.10t. Setauket: Exeter Software.

Roseman CC. 2004. Detection of interregionally diversifying natural selection on modern human cranial form by using matched molecular and morphometric data. Proc Natl Acad Sci USA 101:12824–12829.

Roseman CC, Weaver TD. 2004. Multivariate apportionment of global human craniometric diversity. Am J Phys Anthropol 125:257–263.

Sardi M, Novellino PS, Pucciarelli HM. 2006. Craniofacial morphology in the Argentine Center-West: consequences of the transition to food production. Am J Phys Anthropol 130:333–343.

Sergi S. 1958. Die Neandertalischen palaeanthropen in Italien. In: von Koenigswald GHR, editor. Hundert jahr Neanderthaler. Utrecht: Kemink en Zoon. p 38–51.

Skelton RR, McHenry HM. 1992. Evolutionary relationships among early hominids. J Hum Evol 23:309–349.

Smith HS. 2009. Which cranial regions reflect molecular distances reliably in humans? Evidence from three-dimensional morphology. Am J Hum Biol 21:36–47.

Sparks CS, Jantz RL. 2002. A reassessment of human cranial plasticity: Boas revisited. Proc Natl Acad Sci USA 99:14636–14639.

StatSoft, Inc. 1984–2007. Copyright. Statistica 7. OK: StatSoft, Inc.

Trinkaus E. 1987. The Neanderthal face: evolutionary and functional perspectives on a recent hominid face. J Hum Evol 16:429–443.

Weaver TD, Roseman CC, Stringer CB. 2007. Were Neandertal and modern human cranial differences produced by natural selection or genetic drift? J Hum Evol 53:135–145.

Wood B, Lieberman DE. 2001. Craniodental variation in *Paranthropus boisei*: a developmental and functional perspective. Am J Phys Anthropol 116:13–25.

APPENDIX TABLE. Sample size, geographic and climatic information for the series included in the study

Series	Region	Sample	Longitude	Latitude	Reference point for the geographic coordinates of the series	Temperature (°C)						Rainfall (mm)			
						Annual minimum temperature	Annual maximum temperature	Annual average temperature	Maximum temperature of warmest month	Minimum temperature of coldest month	Temperature range (°C)	Annual rainfall	Rainfall of wettest month	Rainfall of driest month	Relative humidity
New South Wales	Australia	66	151.24	−33.89	Sydney	13.1	22	17.5	26.1	7.1	19	1293	149	61	62
Queensland	Australia	22	144.53	−22.59	Approx. center of Queensland	16.3	31.2	23.7	37	7.9	29.1	481	99	9	40
South Australia	Australia	147	138.61	−34.92	Adelaide	11.2	21.6	16.4	28.6	6.9	21.7	543	77	15	56
West Australia	Australia	28	122.18	−25.49	Approx. Center of Western Australia	15.1	30.2	22.7	38.7	5.8	32.9	212	43	4	32
Kenya	East Africa	95	36.81	−1.27	Nairobi	12.7	24.9	18.8	27.4	11	16.4	904	200	15	67
Malawi	East Africa	26	33.77	−13.98	Lilongwe	14	26.4	20.2	29.9	8.5	21.4	862	224	0	70
Somalia	East Africa	64	45.34	2.03	Muqdisho	23.1	30.7	26.9	32.9	22.1	10.8	480	81	1	68
Tanzania	East Africa	89	35.73	−6.17	Dodomi	16.1	29	22.6	31.6	12.7	18.9	572	129	0	66
Ainu	East Asia	35	141.34	43.05	Sapporo	4.3	12.2	8.2	25.8	−8.6	34.4	1165	140	58	74
Korea	East Asia	33	126.95	37.53	Seoul	7.3	16.4	11.9	29.7	−7.9	37.6	1319	376	20	70
Han North	East Asia	62	123.38	43.8	Sheniang	0.1	12.1	6.1	28.8	−20.5	49.3	457	136	2	63
Han South	East Asia	67	113.64	34.75	Zhengzhou	9	20.1	14.5	32.3	−4.7	37	636	146	7	65
Jomon Japan	East Asia	50	139.82	35.66	Tokyo	11.8	19.5	15.7	30.7	0.9	29.8	1432	185	47	68
Manchuria	East Asia	56	111.43	49.58	Manzhouli	−9	5.3	−1.9	22.6	−28.1	50.7	406	119	3	63
Tohoku Japan	East Asia	107	140.89	38.25	Sendai	8.2	16.1	12.2	28.2	−2.7	30.9	1268	183	51	72
Tokyo Japan	East Asia	43	139.82	35.66	Tokyo	11.8	19.5	15.7	30.7	0.9	29.8	1432	185	47	68
Ancient Italy	Mediterranean	40	12.48	41.89	Rome	10.6	20.7	15.7	30.5	3.7	26.8	798	114	18	73
Badari Egypt	Mediterranean	41	32.67	25.18	El Sibaiya	16.2	33.7	24.9	40.8	6.7	34.1	0	0	0	35
Egypt	Mediterranean	89	31.24	30.06	Cairo	14.2	28.1	21.2	34.7	6.9	27.8	19	5	0	56
Gyzeh, Egypt	Mediterranean	100	31.24	30.06	Cairo	14.2	28.1	21.2	34.7	6.9	27.8	19	5	0	56
Iron Age Israel	Mediterranean	78	35.22	31.77	Jerusalem	11.8	23.2	17.5	30.7	5.3	25.4	511	119	0	64
Iron and Bronze Age Israel	Mediterranean	91	35.22	31.77	Jerusalem	11.8	23.2	17.5	30.7	5.3	25.4	511	119	0	64
Morocco	Mediterranean	30	−6.83	34.01	Rabat	12.9	23	18	28.4	7.7	20.7	521	105	0	77
Naqada Egypt	Mediterranean	80	32.72	25.89	Naqada	15.7	32.9	24.3	40.5	5.6	34.9	0	0	0	40
Recent Greece	Mediterranean	34	23.71	37.97	Athens	13	21.7	17.3	32.5	5.5	27	439	75	5	62
Recent Italy	Mediterranean	101	12.48	41.89	Rome	10.6	20.7	15.7	30.5	3.7	26.8	798	114	18	73
Spain + Portugal	Mediterranean	14	−3.7	40.41	Madrid	9.35	18.9	14.1	27.85	3.3	24.55	821.5	111.5	13	58
Turkey	Mediterranean	52	29	41.06	Istanbul	10.3	17.6	13.9	26.8	2.9	23.9	805	133	26	75
Borneo	Southeast Asia	79	113.31	0.05	Approx. Center of Borneo	19.5	27.9	23.7	28.2	19.2	9	3293	375	166	85
Caroline Islands	Micronesia	22	158.18	6.91	Palikir	22	29	25.5	29.4	21.3	8.1	5113	497	277	84
Easter Papua	Melanesia	21	151.1	−8.49	Trobriand Island	22.9	30.3	26.6	31.6	22.5	9.1	3736	400	194	80
East Sepik, PNG	Melanesia	29	143.61	−3.56	Wewak	22.6	30.9	26.7	31.3	22.1	9.2	2052	206	145	81
Fiji	Melanesia	47	178.43	−18.14	Suva	21.6	27.9	24.8	30.2	19.9	10.3	2999	373	151	76
Gulf Province, PNG	Melanesia	33	145.83	−7.92	Kerema	22.6	30.3	26.4	31.7	21.8	9.9	3376	422	191	80
Java	Southeast Asia	62	106.84	−6.21	Jakarta	22.8	32	27.4	33.2	22.1	11.1	1988	376	67	79
Madang, PNG	Melanesia	33	145.78	−5.23	Madang	22.6	30.3	26.5	30.5	22.2	8.3	3192	388	129	81
Mariana Islands	Micronesia	26	144.74	13.76	Hagatña	23.7	29.3	26.5	30	22.9	7.1	2347	351	91	85
Molucca	Southeast Asia	22	129.45	−3.21	Maluku Island	14.4	20.8	17.6	22.4	13.8	8.6	2760	319	136	82
Negritos Philippines	Southeast Asia	22	120.98	14.6	Manila	23.4	31.3	27.4	33.8	21.6	12.2	2101	456	8	76
New Britain	Melanesia	74	150.7	−5.78	Approx. Center of New Britain	21.6	28.9	25.3	29.9	21	8.9	4081	440	236	80
New Caledonia	Melanesia	51	166.43	−22.29	Nouméa	19.5	26.4	22.9	29.3	16.1	13.2	1029	135	42	76
New Hebrides	Melanesia	52	168.32	−17.34	Port-Vila	20.3	27	23.7	29.3	18.4	10.9	2413	381	110	81
New Ireland	Melanesia	35	152	−3.39	Approx. Center of New Ireland	17.2	24.1	20.7	25	16.8	8.2	2874	304	185	81
Philippines	Southeast Asia	122	120.98	14.6	Manila	23.4	31.3	27.4	33.8	21.6	12.2	2101	456	8	76
Solomon	Melanesia	71	159.94	−9.42	Honiara	22.4	30.2	26.3	30.6	21.5	9.1	2213	346	95	79
Sumatra	Southeast Asia	27	100.35	−0.95	Padang	22.7	31.3	27	31.9	22.5	9.4	4041	493	208	83
Torres Strait	Melanesia	61	142.26	−10.18	Moa Island	23.4	29.8	26.6	31.5	22.1	9.4	1561	339	6	76
West Sepik, PNG	Melanesia	24	141.3	−2.68	Vanimo	22	29.7	25.8	30.4	21.4	9	2558	304	154	80
Early Nubia	North Africa	78	30.47	19.16	Dunqulah	18.5	36.5	27.5	42.9	9.3	33.6	12	8	0	25
Kerma, Nubia	North Africa	86	30.47	19.16	Dunqulah	18.5	36.5	27.5	42.9	9.3	33.6	12	8	0	25
Nubia	North Africa	46	30.47	19.16	Dunqulah	18.5	36.5	27.5	42.9	9.3	33.6	12	8	0	25
Arizona	North America	41	−112.07	33.44	Phoenix	12.9	30.1	21.5	40.8	3.5	37.3	204	28	3	37
Arkansas	North America	29	−92.28	34.74	Little Rock	10.5	22.6	16.6	33.6	−1.2	34.8	1256	133	80	70
Florida	North America	96	−84.28	30.43	Tallahassee	12.9	26	19.5	32.9	4	28.9	1499	193	73	75

APPENDIX TABLE. Sample size, geographic and climatic information for the series included in the study (continued)

Series	Region	Sample	Longitude	Latitude	Reference point for the geographic coordinates of the series	Temperature (°C)						Rainfall (mm)			
						Annual minimum temperature	Annual maximum temperature	Annual average temperature	Maximum temperature of warmest month	Minimum temperature of coldest month	Temperature range (°C)	Annual rainfall	Rainfall of wettest month	Rainfall of driest month	Relative humidity
Illinois	North America	118	−89.64	39.8	Springfield	5.7	17.1	11.4	30.6	−8.6	39.2	912	96	41	71
Kentucky	North America	37	−84.87	34.2	Frankfort	8.8	21.9	15.3	31.5	−1.8	33.3	1334	154	79	70
Maryland	North America	54	−76.49	38.97	Annapolis	8.1	18.5	13.3	30.4	−3.4	33.8	1069	114	71	66
México	North America	73	−99.13	19.41	Mexico city	7.5	24.4	15.9	27.2	2.9	24.3	644	129	7	62
New Mexico	North America	63	−105.93	35.68	Santa Fé	1.1	17.4	9.3	28.8	−9	37.8	395	74	19	46
New York	North America	27	−73.75	42.65	Albany	2.8	14.8	8.8	28.8	−10.8	39.6	946	92	57	70
North California	North America	61	−121.49	38.58	Sacramento	9.1	23.1	16.1	34	3.3	30.7	458	100	1	66
South California	North America	163	−118.24	34.05	Los Angeles	12.5	23.9	18.2	29.2	8.1	21.1	388	88	0	68
South Dakota	North America	119	−100.35	44.36	Pierre	1.7	15.5	8.6	32.2	−14	46.2	427	79	8	64
Utah	North America	58	−111.89	40.76	Salt Lake City	3.5	17.5	10.5	33.1	−7.4	40.5	447	57	20	55
Virginia	North America	58	−77.46	37.55	Richmond	7.5	20.3	13.9	31.2	−3.7	34.9	1097	111	77	70
Buriat	Northeast Asia	27	104.24	52.31	Irkutsk	−5.8	6.1	0.1	24.2	−24.2	48.4	481	113	9	73
Chuckchis	Northeast Asia	21	170.68	65	Approx. Center of Chuktchi Peninsula	−14.7	−3.4	−9	20.4	−32	52.4	351	56	14	86
Mongols	Northeast Asia	151	106.9	47.92	Ulaanbaatar	−7.1	5.6	−0.8	22.9	−26.9	49.8	248	66	2	63
Austria	North Europe	80	16.37	48.2	Wien	5	14.6	9.8	26	−3.8	29.8	631	76	35	73
Czecho	North Europe	95	17.25	49.52	Charvarty	4.1	13.1	8.6	24	−5.1	29.1	586	85	26	77
Ensay	North Europe	67	−7.08	57.76	Ensay Island	5.3	10.5	7.9	15.7	0.8	14.9	1195	137	64	88
Finland	North Europe	25	24.95	60.16	Helsinski	2	8.3	5.1	20.8	−8.8	29.6	649	78	33	80
Germany	North Europe	82	13.4	52.52	Berlin	5	13	9	23.7	−3.4	27.1	574	70	34	79
Hungary	North Europe	93	19.08	47.49	Budapest	6.7	15.4	11	27	−3.3	30.3	562	68	32	70
Lapps	North Europe	34	26.89	67.68	Approx. Center of Lappi	−6	3.2	−1.4	18.6	−20	38.6	492	68	25	78
Netherlands	North Europe	33	4.89	52.37	Amsterdam	6	12.5	9.2	20.7	−0.1	20.8	802	87	43	83
Poundbury, UK	North Europe	102	−2.43	50.71	Dorchester	5.9	13	9.5	20.7	0.9	19.8	827	94	51	86
Recent France	North Europe	63	2.35	48.85	Paris	7.1	15.5	11.3	24.7	0.8	23.9	636	58	44	74
Repton, UK	North Europe	43	−1.47	52.92	Derby	5.9	13.3	9.6	21.1	0.4	20.7	721	71	51	84
Russia	North Europe	44	35.13	48.42	Dnepropetrovsk	4.9	13.4	9.1	27.8	−7.4	35.2	501	59	33	73
Serbia	North Europe	34	20.46	44.8	Belgrade	7.6	17.1	12.3	28.6	−1.5	30.1	663	85	38	69
Spittafields UK	North Europe	57	−0.12	51.5	London	6.9	14.8	10.8	23.2	1.3	21.9	641	62	41	81
Spittafields UK	North Europe	86	−0.12	51.5	London	6.9	14.8	10.8	23.2	1.3	21.9	641	62	41	81
Sweden	North Europe	31	18.07	59.29	Stockholm	3.8	10.3	7	22.2	−4.9	27.1	526	66	25	80
Switzerland	North Europe	37	7.44	46.94	Bern	4.3	12.7	8.5	22.7	−3.2	25.9	944	115	60	76
Ukraine	North Europe	26	34.1	44.96	Kiev	6.1	15.5	10.8	27.5	−3.5	31	516	59	34	74
Alaska	Extreme North America	36	−134.57	58.36	Juneau	1.5	8.5	5	18	−6.7	24.7	1573	228	79	80
British Columbia	North America	78	−123.34	48.44	Victoria	6.2	13.5	9.9	20.1	1.9	18.2	694	116	16	81
East Aleuts	Extreme North America	45	−169.71	52.99	Kagamil Island	2	6.3	4.1	12.7	−3.2	15.9	980	119	56	84
Greenland	Extreme North America	107	−51.72	64.18	Nuuk	−4	1.7	−1.2	10.8	−11.5	22.3	668	78	39	81
Iroques Ontario	North America	40	−79.38	43.67	Toronto	3.7	12.4	8.1	26.5	−9.2	35.7	790	82	52	75
N Alaska	Extreme North America	70	−156.78	71.29	Barrow	−15.3	−9.2	−12.2	7.6	−30.9	38.5	113	25	4	81
Amur	Northeast Asia	22	−170.53	65.84	Pouten	−10.5	−4.6	−7.5	8.3	−24.5	32.8	335	56	16	92
NE Canada	Extreme North America	30	−68.52	63.74	Inqaluit	−13.4	−5.8	−9.6	11.5	−31.1	42.6	406	61	18	75
NW Alaska	Extreme North America	107	−164	65.4	Approx. Center of Seward Peninsula	−8.2	−0.8	−4.5	14.5	−21.6	36.1	357	78	14	76
SW Alaska	Extreme North America	135	−160.45	61	Approx. Southwest Alaska	−5.9	2.7	−1.6	17.6	−19.3	36.9	465	102	19	77
Tlingit Alaska	Extreme North America	35	−134.57	58.36	Juneau	1.5	8.5	5	18	−6.7	24.7	1573	228	79	80
West Aleuts	Extreme North America	82	−166.69	53.7	Aleutian West	1.2	5.6	3.3	12.9	−4.6	17.5	947	111	53	85
Chatam Islands	Polynesia	76	−176.53	−43.91	Chatam islands	8.7	14.4	11.6	18.1	5.2	12.9	904	117	53	
Easter Island	Polynesia	81	−109.36	−27.11	Easter Island	16.2	23.3	19.8	26.6	14	12.6	1160	137	77	79
Hawaii	Polynesia	72	−157.85	21.3	Honolulu	17.7	25.9	21.8	28	15.6	12.4	3298	348	195	69
Marquese Islands	Polynesia	66	−139.56	−8.9	Ua Huka Island	21.9	28.6	25.3	29.5	21.5	8	1276	181	64	
New Zealand	Polynesia	120	174.78	−41.31	Wellington	9.1	16.5	12.8	21.3	5.4	15.9	1166	132	58	81
Society Islands	Polynesia	49	−149.56	−17.53	Papeete	22.7	29.2	25.9	30.6	21.2	9.4	1715	314	50	
Bushman	South Africa	32	18.42	−33.92	Cape town	11.8	21.9	16.8	26.2	7.9	18.3	858	142	25	74
South Africa, Bantu	South Africa	43	28.21	−25.23	Pretoria	11.3	27.3	19.3	30.5	2.8	27.7	582	102	5	58
South Africa	South Africa	24	28.21	−25.23	Pretoria	11.3	27.3	19.3	30.5	2.8	27.7	582	102	5	58
Zulu	South Africa	30	28.21	−25.23	Pretoria	11.3	27.3	19.3	30.5	2.8	27.7	582	102	5	58
Chile	South America	20	−70.64	−33.46	Santiago	7.1	22.1	14.6	29.6	2.6	27	363	87	1	72
Fuego-Patagonia	South America	57	−68.37	−54.09	Approx. Center of	1.4	9	5.2	13.8	−1.8	15.6	437	45	25	76

APPENDIX TABLE. Sample size, geographic and climatic information for the series included in the study (continued)

Series	Region	Sample	Longitude	Latitude	Reference point for the geographic coordinates of the series	Temperature (°C)						Rainfall (mm)			
						Annual minimum temperature	Annual maximum temperature	Annual average temperature	Maximum temperature of warmest month	Minimum temperature of coldest month	Temperature range (°C)	Annual rainfall	Rainfall of wettest month	Rainfall of driest month	Relative humidity
Peru	South America	223	−77.62	−11.11	Tierra del Fuego Huacho	15.4	23.1	19.2	27	13.2	13.8	8	1	0	86
Venezuela + Colombia	South America	12	−74.08	4.61	Bogotá	11.7	22.05	16.9	23	10.1	12.9	901.5	122	26.5	81
Afghanistan	South Asia	40	69.17	34.52	Kabul	4.3	19.3	11.8	32.2	−8.6	40.8	340	82	1	50
Andaman Islands	South Asia	53	92.8	12.47	Andaman Islands	23.9	29.5	26.7	31.7	22.4	9.3	3088	545	6	79
Bangladesh	South Asia	25	90.4	23.7	Dacca	21.3	30.6	25.9	34.5	12.3	22.2	1990	367	7	75
Bengal, India	South Asia	51	88.36	22.57	Kolkata	21.3	31.4	26.3	36.1	12.6	23.5	1730	366	7	71
Bihar, India	South Asia	21	85.13	25.61	Patna	20.8	31.3	26	39	10.9	28.1	1033	289	3	63
Laos	Southeast Asia	32	102.61	17.96	Viang Chan	20.4	30.7	25.5	33.8	13.9	19.9	1635	339	3	75
Madras, India	South Asia	100	80.24	13.06	Chennai	23.8	33.4	28.6	38.5	19.4	19.1	1176	311	2	71
Malaysia	Southeast Asia	56	101.7	3.15	Kuala Lumpur	22.3	31.8	27.1	32.7	21.7	11	2475	285	128	82
Myanmar	Southeast Asia	103	96.15	16.78	Yangon	22.5	32	27.3	36.7	17.9	18.8	2348	507	3	73
Nepal	South Asia	36	85.31	27.7	Katmandu	12.1	24	18.1	28	3.2	24.8	1548	390	8	76
NW India	South Asia	29	77.2	28.63	New Delhi	18.6	31.6	25.1	40.4	7.2	33.2	698	255	3	55
Punjab, India	South Asia	73	73.53	36.73	Approx. Center of Jammu & Kashmir	−8.9	0	−4.4	14.1	−22.8	36.9	267	41	10	51
Sikkim	South Asia	25	88.46	27.6	Approx. Center of Sikkim District	−0.6	11.7	5.5	16.6	−9.7	26.3	833	175	5	74
Singapore	Southeast Asia	43	103.82	1.29	Singapore	22.8	30.8	26.8	31.4	22.1	9.3	2385	297	156	82
Thailand	Southeast Asia	47	100.52	13.73	Bangkok	23.6	32.5	28.1	34.9	20.2	14.7	1414	315	6	75
Tibet	East Asia	64	91.13	29.65	Lhasa	−1.1	13.6	6.3	21.1	−12.1	33.2	379	116	0	50
Vietnam	Southeast Asia	24	105.85	21.02	Hà Noi	20.3	27.4	23.8	33	13.3	19.7	1670	323	16	83
Cameroon	West Africa	33	11.51	3.87	Yaoundé	19.1	28.2	23.6	29.6	18.4	11.2	1659	300	22	79
Gabon	West Africa	76	9.45	0.39	Libreville	23	29.2	26.1	30.6	21.8	8.8	2883	501	2	84
Ghana	West Africa	51	−0.19	5.55	Accra	23.2	30.2	26.7	32	21.6	10.4	803	207	14	82
Ibo, Nigeria	West Africa	79	7.48	9.05	Abuja	19.6	31.2	25.4	34.7	16.6	18.1	1401	287	1	62
Ivory Coast	West Africa	27	−5.28	6.81	Yamoussoucro	20.9	31.1	26	33.8	19.2	14.6	1155	174	14	75
Nigeria	West Africa	45	7.48	9.05	Abuja	19.6	31.2	25.4	34.7	16.6	18.1	1401	287	1	62